THE SCIENCE AND TECHNOLOGY OF INDUSTRIAL WATER TREATMENT

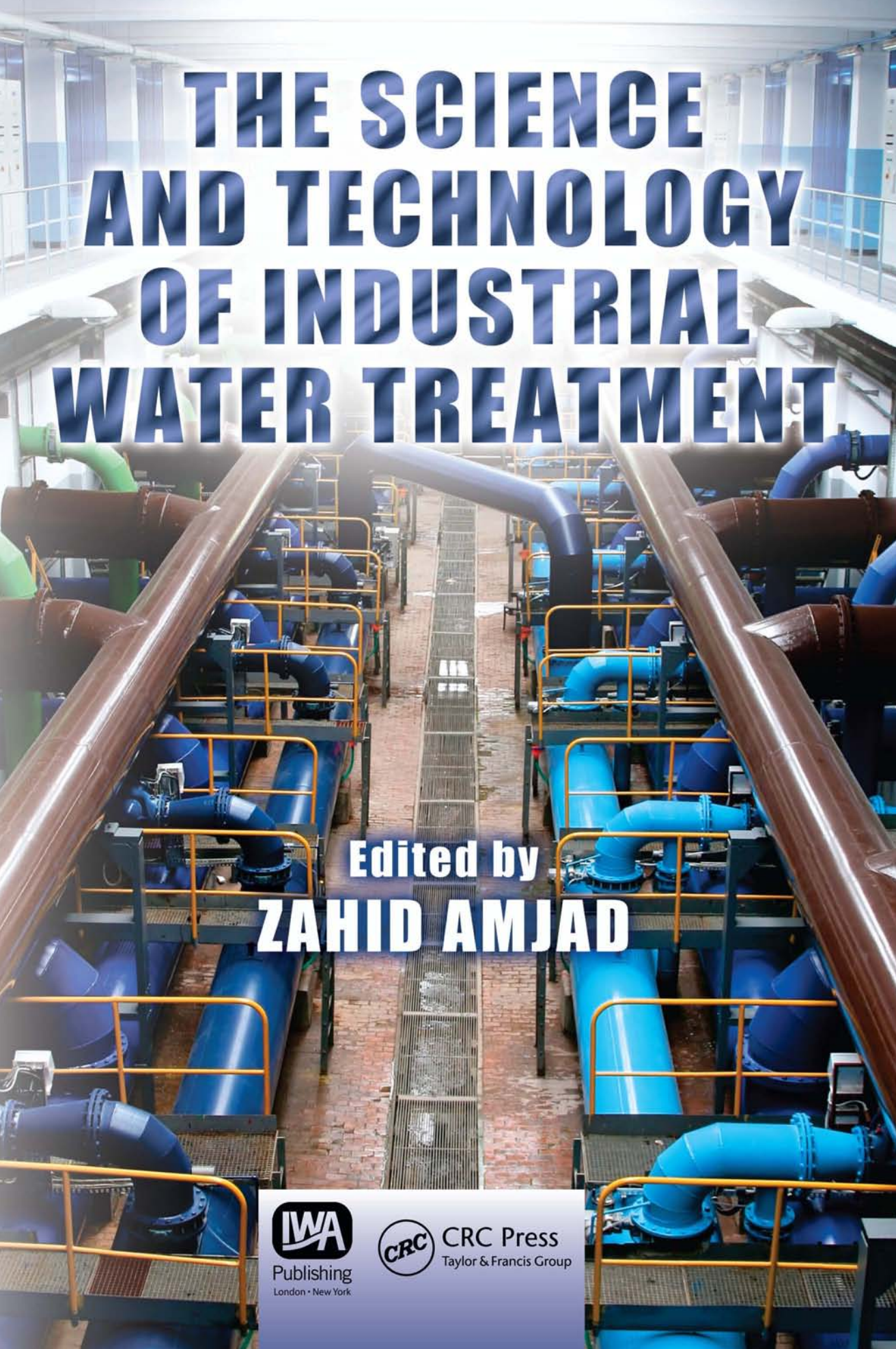

Edited by

ZAHID AMJAD

IWA Publishing
London • New York

CRC Press
Taylor & Francis Group

THE SCIENCE AND TECHNOLOGY OF INDUSTRIAL WATER TREATMENT

Edited by
ZAHID AMJAD

IWA Publishing
London • New York

CRC Press
Taylor & Francis Group
Boca Raton London New York

CRC Press is an imprint of the
Taylor & Francis Group, an **informa** business

Co-published by IWA Publishing, Alliance House, 12 Caxton Street, London SW1H 0QS, UK
Tel. +44 (0) 20 7654 5500, Fax +44 (0) 20 7654 5555
publications@iwap.co.uk
www.iwapublishing.com
ISBN 1843393115
ISBN13 9781843393115

CRC Press
Taylor & Francis Group
6000 Broken Sound Parkway NW, Suite 300
Boca Raton, FL 33487-2742

Printed in the United States of America on acid-free paper
10 9 8 7 6 5 4 3 2 1

International Standard Book Number-13: 978-1-4200-7145-0 (Ebook-PDF)

10 Recent Developments in Controlling Silica and Magnesium Silicate Foulants in Industrial Water Systems

Konstantinos D. Demadis

CONTENTS

10.1 Introduction 179
10.2 Formation and Growth of Amorphous Silica 180
10.3 Silica Scale Control 182
10.4 Silica Growth Inhibition by the Use of Chemical Additives 183
10.5 Mechanism of Silica Scale Inhibition 188
10.6 Magnesium Silicate in Geochemistry 188
10.7 Water-Formed "Magnesium Silicate" Deposits 189
10.8 The Role of Mg^{2+} Level, Temperature, pH, and Supersaturation 191
10.9 Other Metal Silicate Scales 192
10.9.1 Iron Silicate 192
10.9.2 Aluminum Silicate 194
10.9.3 Calcium Silicate 195
10.10 Effect of Other Cations 195
10.11 Magnesium Hydroxide and Its Role in Magnesium Silicate Formation 195
10.12 Effect of Additives on Metal Silicate Scale Control 195
10.13 Practical Guidelines for Control of Magnesium Silicate Scale 197
10.14 "Metal Silicates" in Biological Systems 198
10.15 Epilogue 199
Acknowledgments 199
References 200

10.1 INTRODUCTION

Fouling presents an enormous challenge in industrial process waters [1]. Often system operators are obligated to discard critical equipment components because of fouling and the inability to remove it. Even if mechanical or chemical cleaning are viable options, they require several hours, total system shutdowns, and high costs [2]. Foulants could be organic or inorganic, as illustrated in Figure 10.1. Organic foulants are a result of poor system biocontrol, or deposition of organic matter brought into the system from external sources (e.g., a river or lake) [3]. Inorganic foulants include crystalline sparingly soluble salts such as calcium carbonate(s), calcium sulfate(s), barium, and strontium sulfates, as well as amorphous and colloidal deposits, such as amorphous calcium phosphate, silica, magnesium silicate, and many others, depending on the particular water chemistry [4]. This chapter deals with silica and metal silicate scales and deposits (with an emphasis on magnesium silicate).

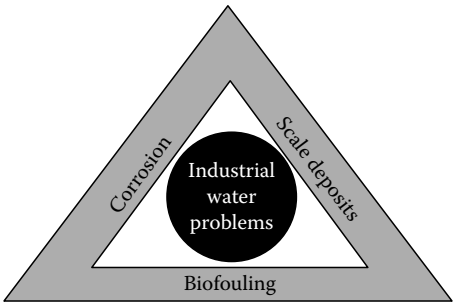

FIGURE 10.1 Schematic depiction of industrial water problems. (Reproduced from Demadis, K.D. et al., *Desalination*, 213, 38, 2007. With permission.)

Silica and magnesium silicate are poorly studied foulants and established methods for their control are not satisfactorily developed. Perhaps the reason for that is their scarcity in water systems; their presence is rather limited to those waters that satisfy one of the following three conditions: (a) contain high levels of silica, (b) contain high levels of magnesium, or (c) operate at high pH regions (>8.5). The purpose of this chapter is to review the "state of the art" of the formation and control of silica and magnesium silicate and to present efforts for their control using chemical additives. Throughout this chapter, the term "soluble silica" means "molybdate-reactive silica."

10.2 FORMATION AND GROWTH OF AMORPHOUS SILICA

The formation, precipitation, and deposition of amorphous silica in process industrial waters have been a subject of intense interest. In parallel, there is also substantial focus on biosilica formation, due to the fact that silica is used by nature as a structural material for several organisms, such as diatoms [5]. Silica scale formation is a highly complex process [6]. It is usually favored at a pH level of less than 8.5, whereas magnesium silicate scale forms at a pH level of greater than 8.5. Available data suggest that silica solubility is largely independent of pH in the range of 6–8. This pH region of minimum silica solubility and silicic acid polymerization has a maximum rate, as shown in Figure 10.2. Silica exhibits normal solubility characteristics. Its solubility increases proportionally to temperature. In contrast, magnesium silicate exhibits inverse solubility. Other forms of silica, e.g., quartz (crystalline SiO_2) and glass also possess "normal" solubility, but they are both less soluble than amorphous silica. This is shown clearly in Figure 10.3.

Silica formation is actually a polymerization event. When silicic acid/silicate ions condense and polymerize, they form a plethora of structural motifs, including rings of various sizes, cross-linked polymeric chains of different molecular weights, oligomeric structures, etc. [7]. The resulting silica scale is a complex and amorphous product (colloidal silica)—a complicated mixture of the above components. Silicic acid polymerization starts with an attack of a deprotonated, negatively charged silicate ion to a silicic acid molecule, yielding an initial "dimer," which then continues to undergo further attack. The initial stages of the silica dimerization/oligomerization/polymerization process are shown in Figure 10.4. This results in random polymer chain growth that produces silica nanoparticles. These, in turn, can further grow (by incorporation of silicic acid onto the silica particle surface) or agglomerate with other nanoparticles to give larger particles.

Operation in a high-pH regime is not necessarily a solution for combating silica scale. Water system operators must take into account the presence of magnesium (Mg^{2+}) and other scaling ions such as calcium (Ca^{2+}). As will be discussed later, other metal cations may aggravate metal silicate fouling. A pH adjustment to greater than 8.5 might result in the massive precipitation of magnesium silicate if high levels of Mg^{2+} are present or in calcium carbonate ($CaCO_3$) or calcium phosphate if high levels of these ions are overlooked.

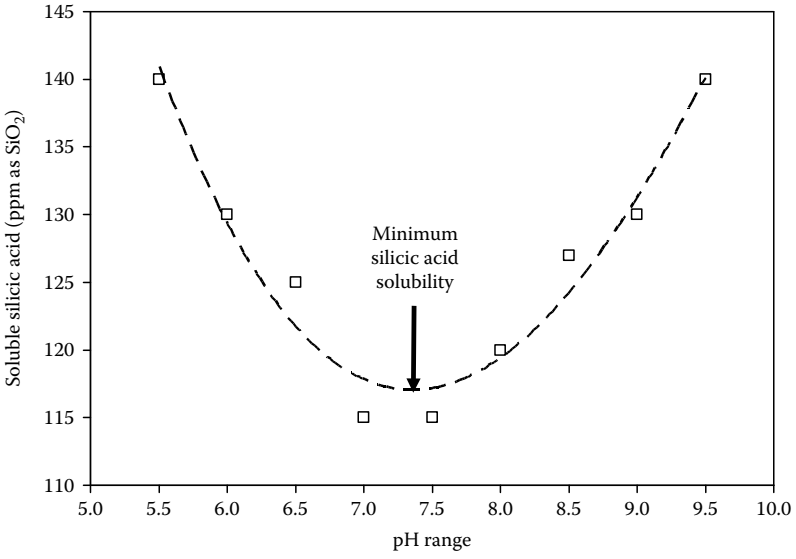

FIGURE 10.2 Dependence of silicic acid polymerization on pH based on experimental results [17j]. Starting level of silicic acid was 500 ppm (as SiO_2) and pH of silica growth was 7.00. (Reproduced from Ketsetzi, A. et al., *Desalination*, 223, 487, 2008. With permission.)

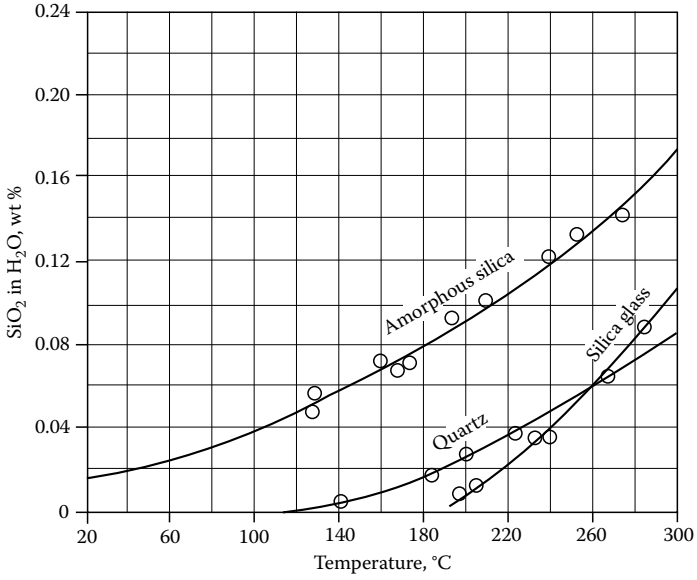

FIGURE 10.3 Dependence of different forms of silica solubility on temperature.

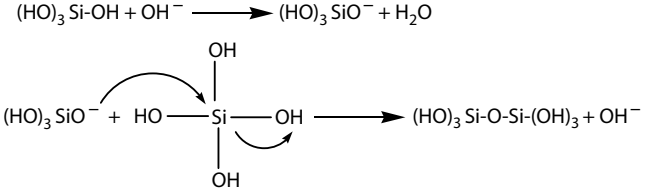

FIGURE 10.4 Initial steps in silicic acid polymerization. (Reproduced from Ketsetzi, A. et al., *Desalination*, 223, 487, 2008. With permission.)

Silica precipitation can also be aggravated by the presence of metal ions such as iron ($Fe^{2+/3+}$) or aluminum (Al^{3+}) and their hydroxides. Corroded steel surfaces (e.g., on pipes or heat exchangers) are prone to silica fouling. Iron oxides/hydroxides act as deposition matrices for silica (either soluble or colloidal) deposits.

There are three principal ways by which silica forms [8]: surface deposition, bulk precipitation, and in living organisms.

Surface deposition: This occurs as a deposit on a solid surface where silicic acid condenses with any solid surface possessing −OH groups. If the surface contains M–OH moieties (M = metal), this reaction is further enhanced. Such pronounced silica deposition phenomena in the water treatment industry are evident on metallic surfaces that have suffered severe corrosion on a surface covered with metal oxides/hydroxides. Once the receptive surface is covered with silica scale, additional silica is deposited on an already formed silica film.

Bulk precipitation: This occurs as colloidal silica particles grow through the aforementioned condensation reaction. The particles collide with each other and agglomerate, forming larger particles.

In living organisms: This form of silica is called biogenic or biosilica and appears in certain microorganisms such as diatoms that have the ability to remove and deposit silica from highly undersaturated solutions into precisely controlled structures of intricate design [9]. It should be mentioned that sessile microorganisms in a biofilm-fouled heat exchanger can entrap colloidal silica. The high affinity of soluble silica toward extracellular biopolymers such as polysaccharides has also been recognized.

10.3 SILICA SCALE CONTROL

The current practices for combating silica scale growth in industrial waters include operation at low cycles of concentration (The number of cycles of concentration indicated how many times the concentration of a certain water-soluble species has been increased.), prevention of "other" scale formation, pretreatment [10], and inhibitor or dispersant use. This section focuses on the inhibition of silica polymerization by the use of polymers.

Operation at low cycles of concentration is a common practice, but one that consumes large amounts of water. In a cooling tower operating at a pH level of less than 7.5, soluble silica generally should be maintained below 200 ppm (as SiO_2). For a pH level higher than 7.5, soluble silica should be maintained below 100 ppm (as SiO_2). One should bear in mind that Mg^{2+} levels also should be taken into account at a pH level greater than 7.5. In this case, the product (ppm Mg as $CaCO_3$) × (SiO_2 as SiO_2) should be below 20,000.

Prevention of "other" scale formation indirectly interferes with the propensity of silica scale to co-precipitate with other scales [11]. The method is based on the prevention of other scaling species such as $CaCO_3$ or calcium phosphate and indirectly benefits the whole cooling tower operation. $CaCO_3$ precipitates provide a crystalline matrix in which silica can be entrapped and grown. In environments in which $CaCO_3$ or any other mineral precipitate is prevented completely, higher silica levels generally are tolerated in the process water as opposed to those environments in which other scales are controlled ineffectively.

Pretreatment involves reactive or colloidal silica removal in precipitation softeners through an interaction between silica and a metal hydroxide. Both iron hydroxide, $Fe(OH)_3$, and aluminum hydroxide, $Al(OH)_3$, have shown silica-removal capabilities, although magnesium hydroxide, $Mg(OH)_2$, is considered to be more effective. In addition, silica can be removed through reverse osmosis (RO) and ion exchange techniques, as well as desilicizers. RO membranes are not immune to silica scale, which forms as a gelatinous mass on the membrane surface. It can then dehydrate, forming a cement-like deposit [12].

10.4 SILICA GROWTH INHIBITION BY THE USE OF CHEMICAL ADDITIVES

The use of inhibitors or dispersants to control silica scale generally follows two approaches: (a) inhibition and (b) dispersion. Inhibition is defined as the prevention of silicic acid oligomerization or polymerization. As a result, silicic acid remains soluble and, therefore, formation of colloidal silica is prevented. Dispersion, on the other hand, is the prevention of particle agglomeration to form larger-size particles and the prevention of the adhesion of these particles onto surfaces.

A number of products are available commercially for silica scale control in RO, geothermal, and evaporative cooling water applications. A detailed discussion of these commercial products is not the intent of this chapter. However, some promising chemistries will be discussed herein. Much information about commercial silica scale treatment can be found on the Internet through any of the popular search engines. In addition, several proprietary technologies can be found in patent literature.

Amjad et al. [13] have tested a number of polymers for silica inhibition with an emphasis on reverse osmosis systems. They discovered that a proprietary polymer at a polymer:silica ratio of 1:12 can maintain ~500 ppm of soluble silica in a pilot scale RO system for about 5 h. The conditions of the study were 600 ppm initial silica, 200 ppm Ca, 120 ppm Mg, and pH 7 at 40°C. A mixture containing molybdate (MoO_4^{2-}), phosphonate (diethylenetriamine-penta(methylene-phosphonic acid), and a copolymer of acrylic acid and 2-acrylamido-2-methylpropane sulfonic acid (AA:SA) was found to be effective in preventing the formation and deposition of silica-containing deposits [14]. A carboxylate/sulfonate/balanced terpolymer was tested in the field [15]. This multipolymer contains balanced hydrophilic/hydrophobic functional groups that enhance adsorption of the dispersant onto colloidal silica and magnesium silicate composite scales when the temperature is raised. In addition, the multipolymer contains sulfonate and carboxylate groups that impart tolerance to soluble iron and superior dispersancy. The presence of the hydrophilic groups serves to induce steric repulsion between silica particles that have polymer chains adsorbed onto them. In another study, a polyanionic/neutral polymer at 12.5 ppm maintained soluble silica up to 370 ppm in RO systems [16].

Recent research in our laboratories has shown that "small molecules" (cationic or anionic) are not active in silica scale inhibition under conditions and dosages pertinent to water treatment systems [17]. Furthermore, anionic polymers have also shown inactivity; one literature example showed that modified polyacrylates (at dosages >1000 ppm) have shown some inhibition [18]. Therefore, polymeric additives that contain some degree of cationic charge were sought. The schematic structures of some inhibitors are shown in Figure 10.5.

The selected polymers show a variety of structural features. All contain some degree of cationic charge. Some (PAMAM-1, PAMAM-2, PEI, PALAM, PAMALAM) possess cationic charge exclusively. Others (PPEI, PCH) are zwitterionic, i.e., they have cationic and anionic charge on the polymer backbone. Some polymers possess a positive charge by virtue of the protonated amine groups (PAMAM-1, PAMAM-2, PEI, PALAM), while others have a "pure" cationic charge due to a tertiary N group (PAMALAM). These additives have been extensively tested with varying dosages. Figure 10.6 presents silicic acid stabilization results with 40 ppm dosage for all polymers.

It is evident from Figure 10.6 that all polymers show inhibitory activity (higher soluble silicate levels than the "control" [17]). PAMAM-1 and PAMAM-2 (both have their surface amine groups protonated at pH 7) are very effective inhibitors at a dosage of 40 ppm. The presence of protonated amine groups is not the only necessary condition for good inhibition. Notice that polymers PEI and PALAM (also having their amine groups protonated at pH 7) show rather poor performance. This could be explained by the fact that excessive cationic charge causes the polymeric additive to be entrapped and hence deactivated within the colloidal silica matrix. PAMALAM, which is a polymer that possesses a tertiary N group, is a "medium" performance inhibitor. From the zwitterionic polymers (PPEI and PCH), PPEI is a very effective inhibitor. In this case, it appears that the negative charge ($-PO_3H^-$ for PPEI) "balances" the positive charge in such a way that the polymer continues to be active, but inhibitor entrapment and deactivation is stopped. For the PCH polymer, perhaps the anionic charge (due to $-PO_3H^-$) is too excessive and the cationic charge (necessary for inhibition) is "neutralized."

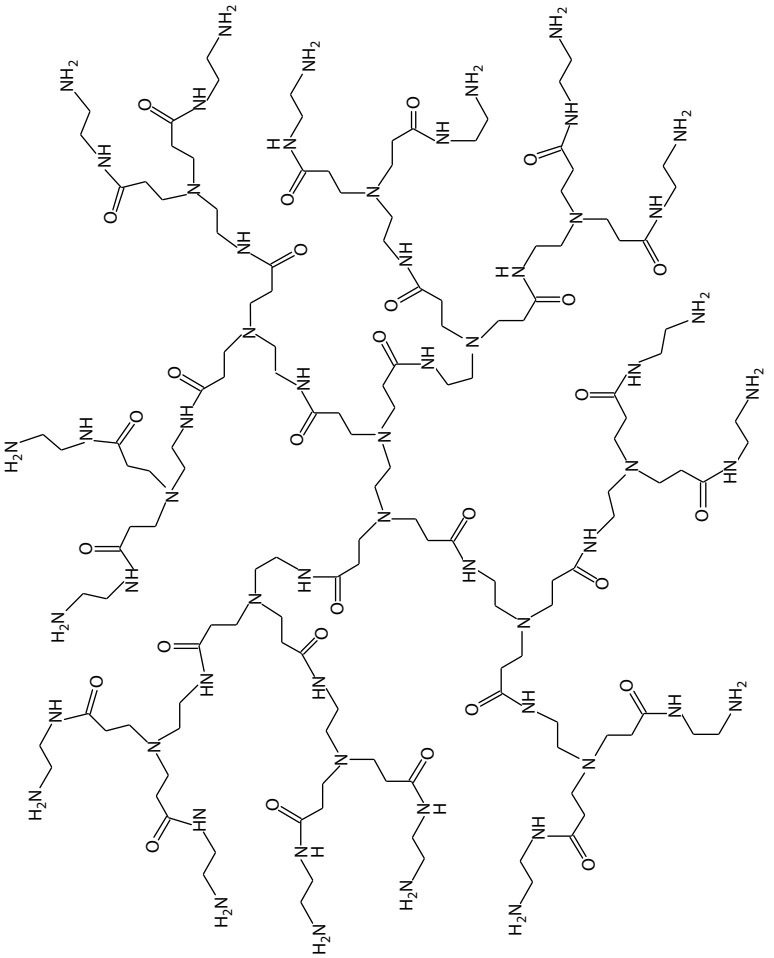

PAMAM-2

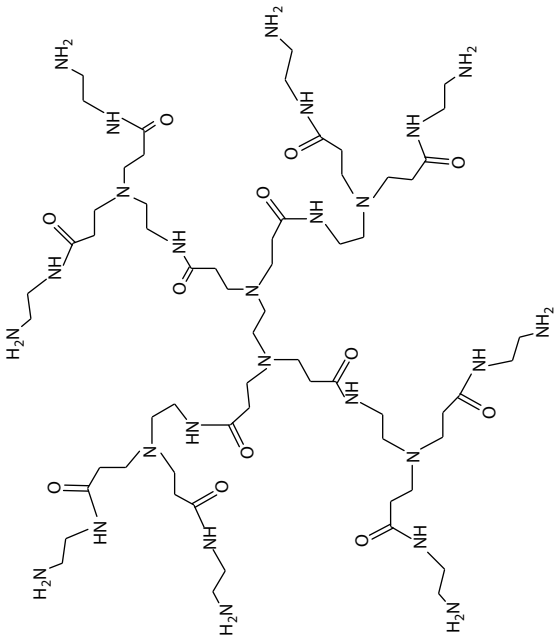

PAMAM-1

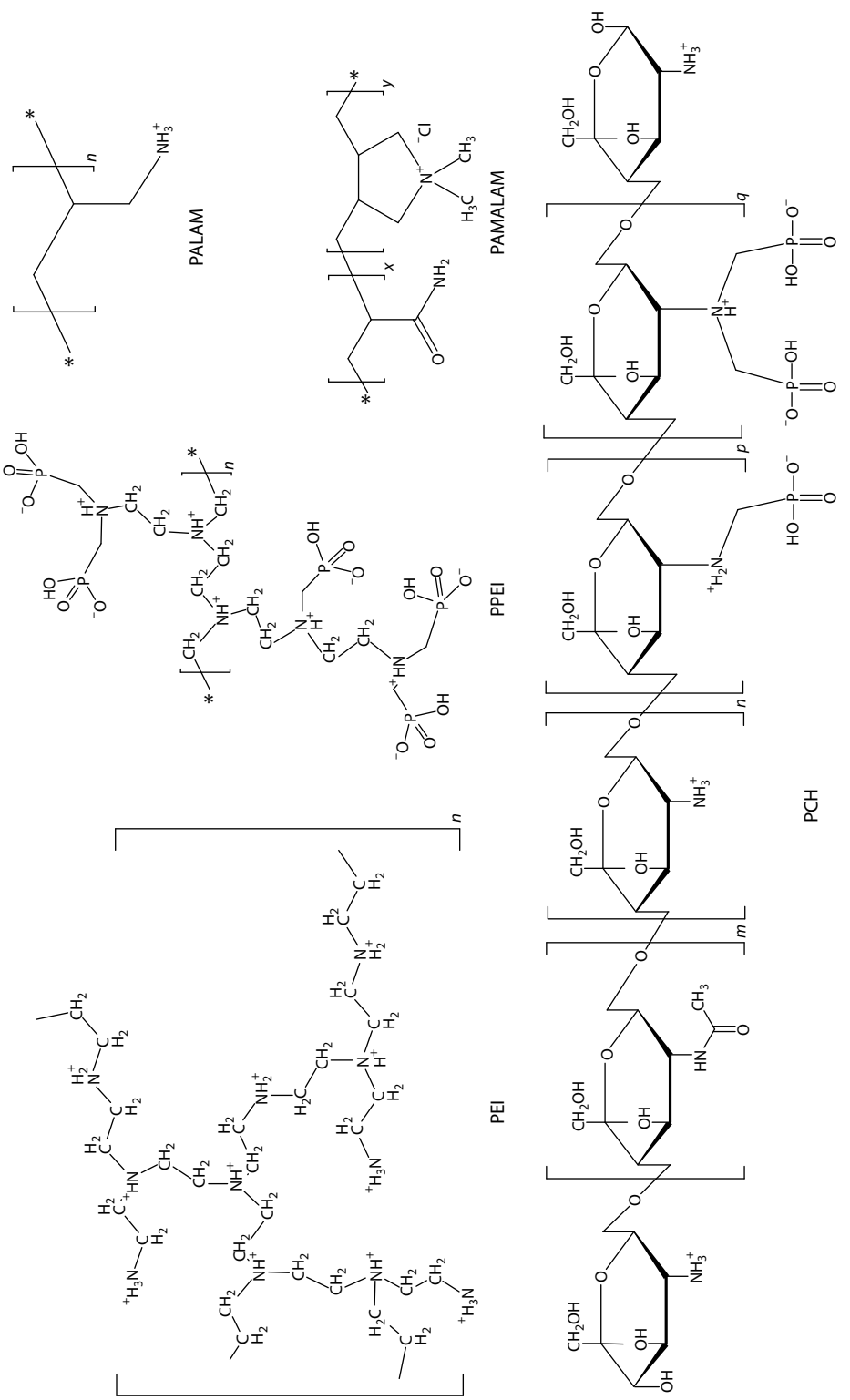

FIGURE 10.5 Schematic structures of the polymeric inhibitors. Abbreviations: PAMAM-1, polyaminoamide dendrimer of generation 1; PAMAM-2, polyaminoamide dendrimer of generation 2; PEI, polyethyleneimine; PALAM, polyallylamine; PAMALAM, poly(acrylamide-*co*-diallyl-dimethylammonium chloride) ($x = 0.55$, $y = 0.45$); PPEI, phosphonomethylated PEI; PCH, phosphonomethylated chitosan with $m = 0.16$, $n = 0.37$, $p = 0.24$, $q = 0.14$.

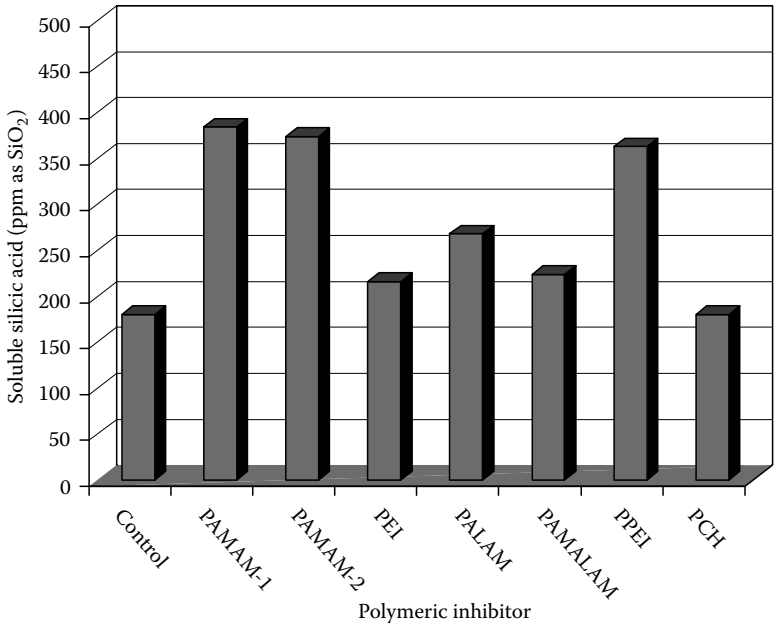

FIGURE 10.6 Silicate stabilization (starting silicate level = 500 ppm) in the presence of polymeric additives (at 40 ppm dosage). Experimental conditions: pH = 7.0, temperature = 2.5°C, polymerization time = 24 hours, filter pores 0.8 µm.

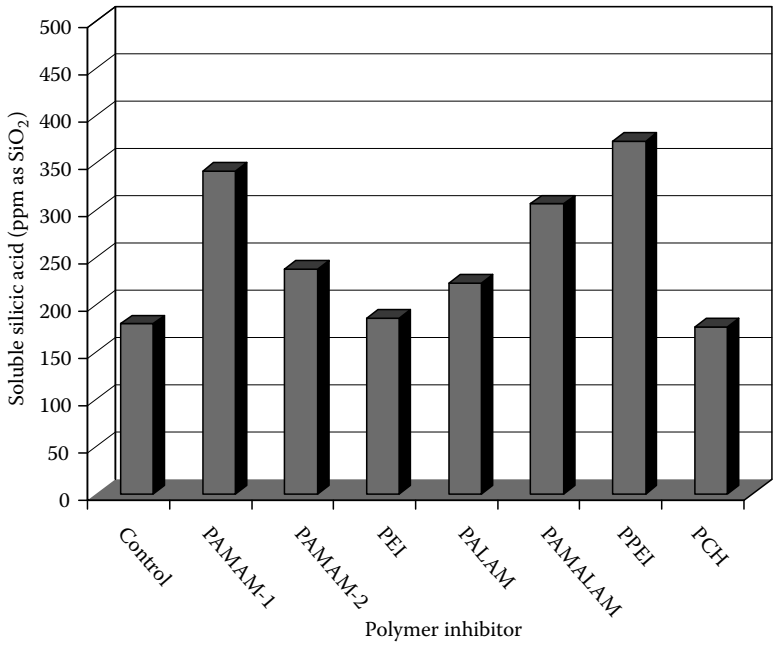

FIGURE 10.7 Silicate stabilization (starting silicate level = 500 ppm) in the presence of polymeric additives (at 80 ppm dosage) (The experimental conditions are the same as in Figure 10.6).

When the polymer dosage is doubled (an increase from 40 to 80 ppm), a number of interesting features appear in the inhibition activity (Figure 10.7). PAMAM-1 retains its inhibitory activity, in contrast to PAMAM-2, which substantially drops in performance (from 374 to 238 ppm soluble silicate). PEI, PALAM, PPEI, and PCH retain their previous inhibitory activity, with only minor alterations. The only polymer that increases its activity is PAMALAM. Further dosage increase, however, caused no further solubility enhancement (data not shown).

It is apparent that an increase in inhibitor dosage has detrimental effects on inhibitory activity. This has been observed before for other cationic inhibitors [17c]. It can be explained upon the examination of the possible silica inhibition mechanism. Experimental results from our group have supported the premise that anionic molecules (either monomeric or polymeric) have no effect on silicate polymerization [17c]. In contrast, cationic polymeric molecules are effective silica scale inhibitors [17]. When silicate polymerization takes place in the presence of a cationic polymeric additive, there are a number of competing reactions taking place concurrently: (a) polymerization of silicic acid. This occurs through an S_{N^2}-like mechanism that involves the attack of a monodeprotonated silicic acid molecule on a fully protonated silicic acid molecule. This pathway generates at first short-lived silicate dimers, which in turn continue to polymerize in a random way to eventually yield colloidal silica particles. (b) Silicate ion stabilization by the cationic additive. This is the actual inhibition step and occurs presumably through cation–anion interactions, and (c) flocculation between the polycationic inhibitor and the negatively charged colloidal silica particles (at pH 7) that are formed by the uninhibited silicate polymerization (Figure 10.8).

The cationic inhibitor is trapped within the colloidal silica matrix, based on process (c). This is demonstrated by the appearance of a light flocculent precipitate (or dispersion at times). Inhibitor entrapment causes its depletion from solution and its deactivation. Therefore, only a portion of the inhibitor is available to continue inhibition at much lower levels than initially added to the polymerization medium. Thus, soluble silicate levels continue to decrease because eventually there is not a sufficient amount of inhibitors to perform the inhibition. Inhibitor entrapment is directly

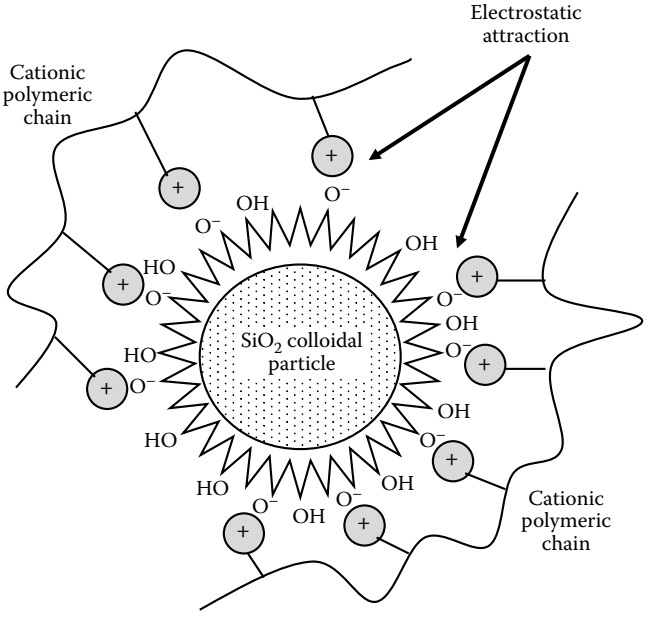

FIGURE 10.8 Cationic polymer–induced flocculation of silica particles that leads to inhibitor entrapment. (Reproduced from Ketsetzi, A. et al., *Desalination*, 223, 487, 2008. With permission.)

proportional to cationic charge density. For example, PEI (polyethyleneimine), a branched cationic polymer with high positive charge density, creates composite precipitates with colloidal silica rapidly [17f]. It is now certain that effective silica scale inhibition is dependent on the cationic charge on the polymer backbone (in an as of yet insufficiently quantified fashion). It has been demonstrated that certain cationic polymers are trapped in the colloidal silica matrix by FT-IR spectroscopy and elemental analyses [17c].

10.5 MECHANISM OF SILICA SCALE INHIBITION

Amorphous silica formation is governed by several important equilibria. Some of these are given in Figure 10.9.

As mentioned above, silica deposition results from silicic acid self condensation. This reaction is first order and is catalyzed by OH^- in the pH range of 5–10. Reports have shown that the reaction yielding a silicic acid dimer is kinetically slow in contrast to the reactions giving a trimer, tetramer, pentamer, etc., which are very fast [19]. All these equilibria are sensitive to pH and tend to be accelerated by metal ions that form hydroxides, e.g., $Fe^{2+/3+}$, Mg^{2+}, or Al^{3+}.

Polymerization of silicic acid is believed to occur through a S_N2-like mechanism involving a deprotonated silicic acid monoanion ($(HO)_3Si\text{-}O^-$) and the Si center of silicic acid, $Si(OH)_4$. Inhibition of this step should be critical in the inhibition of silica scale formation. Some reports indicate that orthosilicates hydrolyze more rapidly than other silicate species such as disilicates, chain silicates, cross-linked oligomers, and polymers, suggesting that bridging oxygens are much more resistant to attack than non-bridging oxygens. Above a pH of 2, this mechanism involves polymerization with condensation, catalyzed by OH^-.

One can envision electrostatic interactions between a cationic polymeric inhibitor and monodeprotonated silicic acid. These interactions stabilize soluble silicate and prohibit the condensation reaction. Alternatively, a cationic polymer whose positive charge is primarily based on protonated amine moieties can stabilize silicic acid molecules and/or silicate ions by hydrogen bonds. Most likely, a combination of the above interactions occur simultaneously for polymeric inhibitors with protonated amine groups, whereas electrostatic interactions are responsible for the stabilizing effect for polymers that have no N–H moieties, but possess $-NR_4^+$ groups (e.g., PAMALAM).

To prove that cationic charges on the polymer backbone are responsible for the silicic acid stabilizing effect, experiments were performed in which a second, anionic polymer was added with the cationic polymeric inhibitor. If this second anionic polymer is added in sufficient excess to "blanket" the positive charge of the cationic inhibitor, inhibition performance deteriorates to virtually none [20]. This was proven for dendrimers PAMAM-1 and PAMAM-2 and PCH. The characteristics of the anionic polymer play a profound role in this "inhibition of inhibition" event.

The precise mechanism of silica formation is only partially understood. As a consequence, the exact mechanism of silica scale inhibition is not fully delineated. However, it is now certain that any interference with the condensation reaction could lead to silica scale growth inhibition. A relevant example is silica inhibition by orthoborate, which reacts with silicate ions to form borosilicates. These products are more soluble in water than are silica/metal silicates [21].

$$Si(OH)_4 \leftrightarrow [SiO(OH)_3]^- + H^+$$

$$Si(OH)_4 \leftrightarrow [SiO_2(OH)_2]^{2-} + 2H^+$$

$$2Si(OH)_4 \leftrightarrow Si_2O(OH)_6 + H_2O$$

$$2Si(OH)_4 \leftrightarrow [Si_2O_2(OH)_5]^- + H_2O + H^+$$

$$2Si(OH)_4 \leftrightarrow [Si_2O_3(OH)_4]^{2-} + H_2O + 2H^+$$

FIGURE 10.9 Silicic acid equilibria that occur in aqueous systems.

10.6 MAGNESIUM SILICATE IN GEOCHEMISTRY

Examination of the composition of the nine rock-forming minerals reveals that they all belong to the silicate group of minerals. The basic building unit of silicate minerals is the SiO_4^{4-} complex ion, the silicon tetrahedron. Oxygen and silicon are the most

TABLE 10.1
Names and Compositions of the Most Common Magnesium Silicate Minerals

Magnesium Silicates	Molecular Formula
Chrysotile	$Mg_3Si_2O_5(OH)_4$
Clinoenstatite	$Mg_3Si_2O_6$
Enstatite	$Mg_2Si_2O_6$
Forsterite/chrysolite	Mg_2SiO_4
Magnesiosilica	$MgOSiO_2$
Olivine	$Mg_{1.6}Fe^{2+}(SiO_4)$
Orthochrysotile	$Mg_3Si_2O_5(OH)_4$
Parachrysotile/amianthus	$Mg_3Si_2O_5(OH)_4$
Pyrope	$Mg_3Al_2(SiO_4)_3$
Ringwoodite	Mg_2SiO_4
Saponite	$Ca_{0.1}Na_{0.1}Mg_{2.25}Fe^{2+}_{0.75}$ $Si_3AlO_{10}(OH)_2{\cdot}4H_2O$
Sepiolite	$Mg_4Si_6O_{15}(OH)_2{\cdot}6H_2O$
Serpentine/clinochrysotile	$Mg_3Si_2O_5(OH)_4$
Stevensite	$Ca_{0.15}Na_{0.33}Mg_{2.8}Fe^{2+}_{0.2}$ $Si_4O_{10}(OH)_2{\cdot}4H_2O$
Talc	$Mg_3Si_4O_{10}(OH)_2$
Wadsleyite	$Mg_{1.5}Fe^{2+}_{0.05}SiO_4$

abundant elements in the crust and mantle, and they form the strongly coordinating species SiO_4^{4-} over a wide range of conditions. This species is even stable in silicate melts, and because more than 90% of the Earth's crust is made of these two elements (more than 70% by weight), it is easy to understand why practically all the minerals in the crust (and mantle) are composed of silicate tetrahedra with a variety of other elements included among them.

Although the nine rock-forming minerals were mentioned above, they are really families of minerals with the same structural styles (in fact three of the rock-forming minerals, albite, orthoclase, and plagioclase are all from the feldspar family). In each of these "families" there is a basic framework/geometric arrangement of silicate tetrahedra, and the difference between "family members" is primarily in the types and abundances of other chemical elements that participate in the structure. Table 10.1 shows the most common magnesium silicate minerals.

10.7 WATER-FORMED "MAGNESIUM SILICATE" DEPOSITS

The term "magnesium silicate" is widely recognized in the water treatment industry. However, its definition differs from that in geology. In general, a deposit that contains both magnesium and silicon is called "magnesium silicate." In more harsh environments, such as in geothermal applications, the effect of high temperature favors the formation of geologically recognized magnesium silicates.

Precipitation of magnesium silicate can cause problems in a number of water treatment applications from truck radiators to geothermal wells and plants. Figure 10.10 shows a heat exchanger tube bundle fouled with magnesium silicate. The magnesium silicate system is highly pH-dependent. Below pH 7, there is essentially no chance of precipitation, because the silica exists in an unreactive, non-ionized form. Above pH 9, magnesium silicate is very likely to form because silica forms reactive silicate ions. Furthermore, the temperature is extremely important. Precipitation begins at a lower pH if the temperature is sufficiently high.

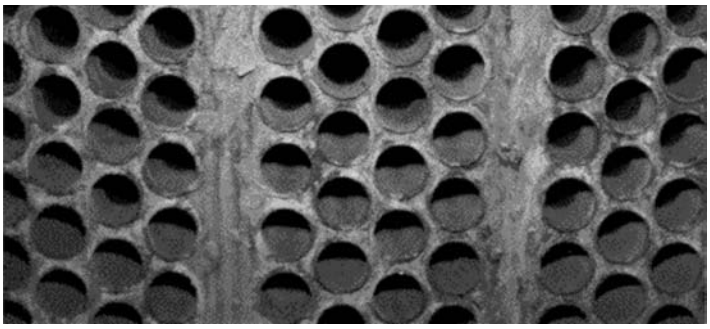

FIGURE 10.10 A magnesium silicate fouled heat exchanger tube bundle.

Scaling of magnesium silicates has been a problem in some of the Icelandic district heating systems [22]. This kind of scaling is not encountered in heating systems utilizing geothermal water directly but occurs by heating and deaerating fresh water. Two of the plants have heat exchangers to heat fresh water. The water in those systems is also discarded after a single use and not recirculated in the heating system. Scaling of a similar type occurred in a few other systems due to the mixing of cold water with the geothermal water. Magnesium silicates have low solubility in warm waters at a high pH level. The heating of groundwater depletes the magnesium concentration of geothermal waters mostly below 0.1 mg/kg. Magnesium silicate is amorphous based on x-ray diffraction (XRD) experiments whatever structure and its resembles that of chrysotile. It was also found that the Mg:Si ratio is close to 1 with small variations. An FT-IR spectrum of the above magnesium silicate deposits is shown in Figure 10.11.

The magnesium silicate sepiolite will precipitate from sea water at low temperatures (down to 25°C), as the dissolved silica concentration is increased. Increased temperature and high pH levels will enhance the rate of precipitation. The magnesium silicate talc will form easily in hydrothermal experiments and is frequently formed outside its stability field. Several other magnesium silicates such as stevensite, saponite, and chrysotile are known to be formed hydrothermally at relatively low temperatures. The heating of fresh water also initiates precipitation and it is well known that magnesium is one of the major components in "boilerstone." The major factors controlling the

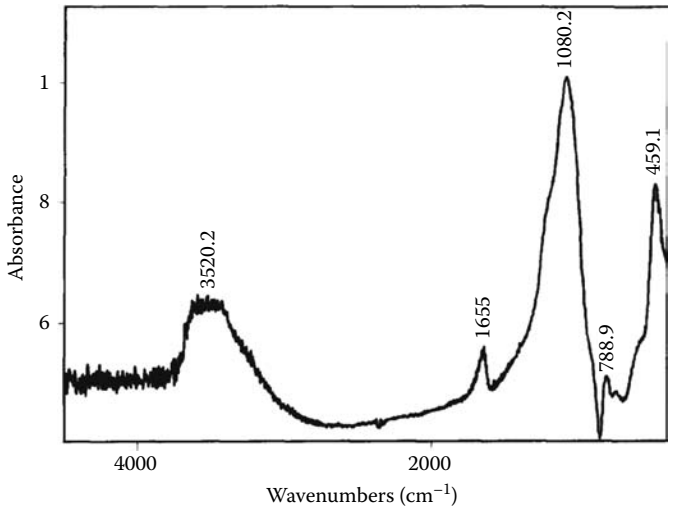

FIGURE 10.11 The FT-IR spectrum of a magnesium silicate deposit from Icelandic water used for heating applications. (Reproduced from Kristmanndóttir H. et al., *Geothermics*, 18, 191, 1989. With permission.)

degree of supersaturation are boiling temperature and pH, which in turn is mainly dependent on the deaeration process. Supersaturation is in all cases greater for talc than for chrysotile [23].

Co-precipitation of magnesium hydroxide, $Mg(OH)_2$, and colloidal silica has also been observed [21]. One theory proposes that the formation of $Mg(OH)_2$ occurs first, and then $Mg(OH)_2$ subsequently reacts with monomeric silicate and/or polymeric silica to form magnesium silicate [24]. Ca^{2+} and Mg^{2+} salts were found to catalyze the silica polymerization reaction [25]. Higher concentrations of total hardness lead to a faster drop in dissolved silica in solution. In batch runs, Mg^{2+} was found to affect silica concentrations more than Ca^{2+}. For example, runs with a given hardness level but with lower ratios of Ca:Mg caused a faster decline in dissolved silica.

Magnesium silicate seems to be a "true" compound according to Young et al. [26]. According to their results, fairly consistent *amorphous* precipitate was obtained. The stoichiometric ratio of silicon to magnesium was found to be 1:1. This is the same whether the mother liquor contained a 1:2 or 2:1 mole ratio of silica to magnesium and whether the precipitation took place at room temperature or 75°C. Some comments on the possible mechanism of formation are warranted. If magnesium hydroxide precipitated out and silica simply absorbed, there should be little effect of silica on the precipitation point. By the same reasoning, the "opposite" mechanism of silica precipitation followed by magnesium absorption should be independent of magnesium concentration. In fact, increasing or decreasing silica concentration has an effect essentially equal to similar increases or decreases in magnesium concentration. The precipitate was found to contain significant amounts of adventitious water, presumably in the pores of the gel. This magnesium silicate precipitate dissolved in acid. Alternatively, ethylenediamine tetraacetic acid chelated the magnesium from the precipitate, leaving a loose flock of virtually pure colloidal silica, which did not redissolve in acid. It can be assumed that the magnesium silicate initially forms a loose, open gel structure with numerous hydroxide bridges. An alternative mechanism of magnesium silicate formation was proposed. According to this proposal, formation of magnesium silicate seems to be a two-step process. Under relatively high pH conditions, magnesium hydroxide is precipitated. Because magnesium hydroxide is inversely soluble with respect to temperature, the precipitation can take place near the surface of the heat transfer tubes and the maximum exchanger tube wall temperature should be ~80°C. Temperature has a greater influence upon the deposition than any of the variables. It was reported that a hydroxylated magnesium silicate forms in seawater in which SiO_2 concentration exceeds 26 ppm at pH 8.1 and clay minerals are found (kaolinite, glauconite, and montmorillonite) [27].

10.8 THE ROLE OF Mg^{2+} LEVEL, TEMPERATURE, pH, AND SUPERSATURATION

Magnesium silicate exhibits "inverse solubility" properties; its solubility decreases as the temperature increases [22,28]. The effect of pH is also profound. At pH regions <8, magnesium is rarely observed in deposits. This does not imply the absence of Si-containing scale deposits, it merely means that magnesium is not incorporated in the deposit structure. Figure 10.12 demonstrates that at pH > 8.5, analyses of several deposits showed that the Mg content increased with pH.

Several experiments performed in our laboratories demonstrated that Mg^{2+} ions actually act as a catalyst in silicic acid condensation reaction. In these experiments, the effect of Mg^{2+} level and pH were studied by following soluble levels of silicic acid. Figure 10.13 clearly shows that at pH 8, Mg^{2+} up to 100 ppm has virtually no effect in the silicic acid condensation reaction.

When pH is increased to 9.0 (Figure 10.14), the catalytic effects of Mg^{2+} start appearing, but Mg^{2+} dosage seems to have no measurable effect.

An increase in the operational pH level to 9.5 has a dramatic change on the catalytic effects of Mg^{2+}. Figure 10.15 demonstrates this dramatic effect. Another significant conclusion derived from Figure 10.15 is that at pH 9.5, the level of Mg^{2+} is now measurable and important. There seems to be a rapid decrease in soluble silicic acid levels as Mg^{2+} concentrations increase. At a level of 100 ppm Mg^{2+}, soluble silicic acid levels drop ~100 ppm lower than the "control." This is convincing evidence that Mg^{2+} is an effective catalyst of silicic acid polymerization at pH regions > 9.0.

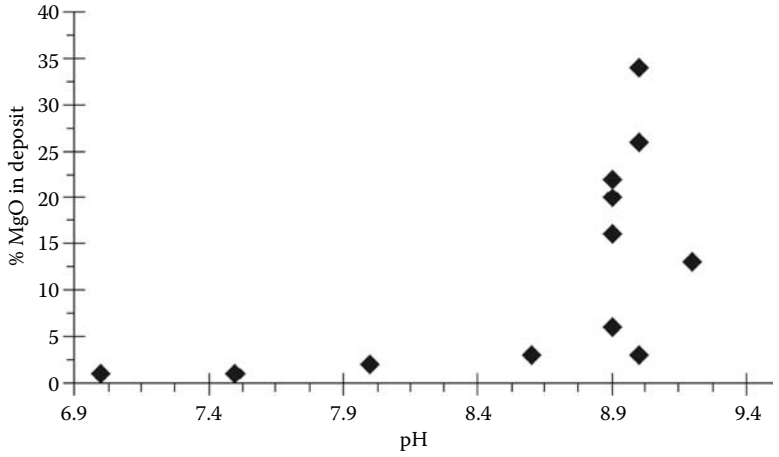

FIGURE 10.12 Magnesium content dependence on operational pH in a magnesium silicate scale deposit from pilot cooling tower tests. (Reproduced from Demadis, K.D. et al., *Desalination*, 179, 281, 2005. With permission.)

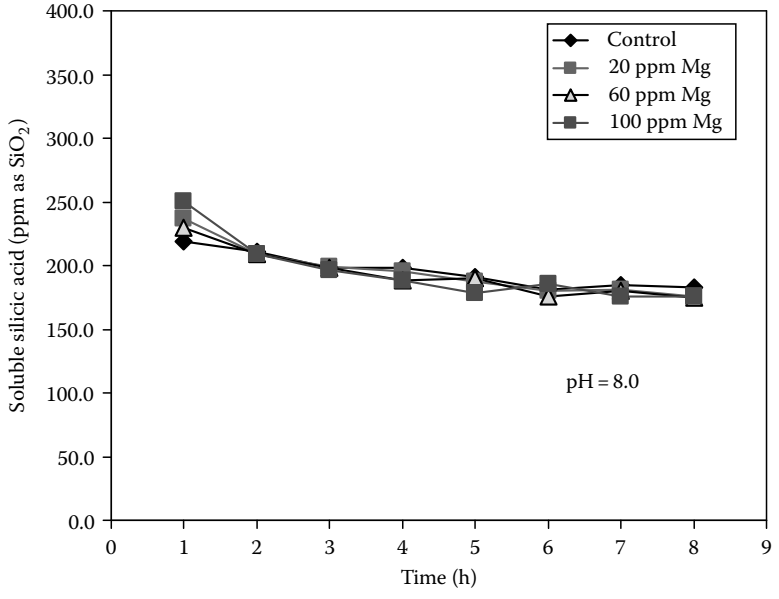

FIGURE 10.13 The effect of Mg level on silica polymerization at pH 8.0.

10.9 OTHER METAL SILICATE SCALES

10.9.1 Iron Silicate

Qualitative evidence for the interaction of silicic acid with metal ions in aqueous solutions was observed as early as 1933 by Mattson [29], who suggested the existence of simple Al-silicate complexes in order to explain his soil experiments. This was followed by Hazel, who employed titrimetric procedures to study metal–silicate interactions with metals such as Al, Fe, and Cr [30]. No quantitative relationships were established for any of these interactions until the work of Weber and Stumm delineated the formation of a Fe(III)-silicate complex [31]:

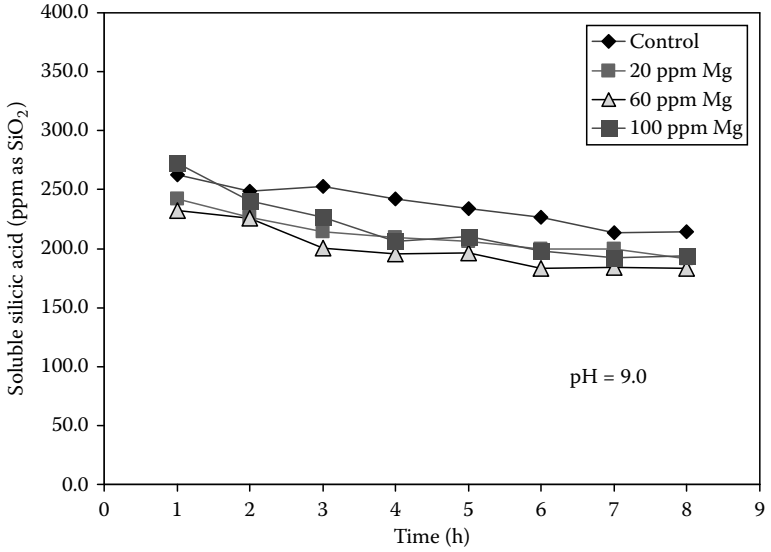

FIGURE 10.14 The effect of Mg level on silica polymerization at pH 9.0.

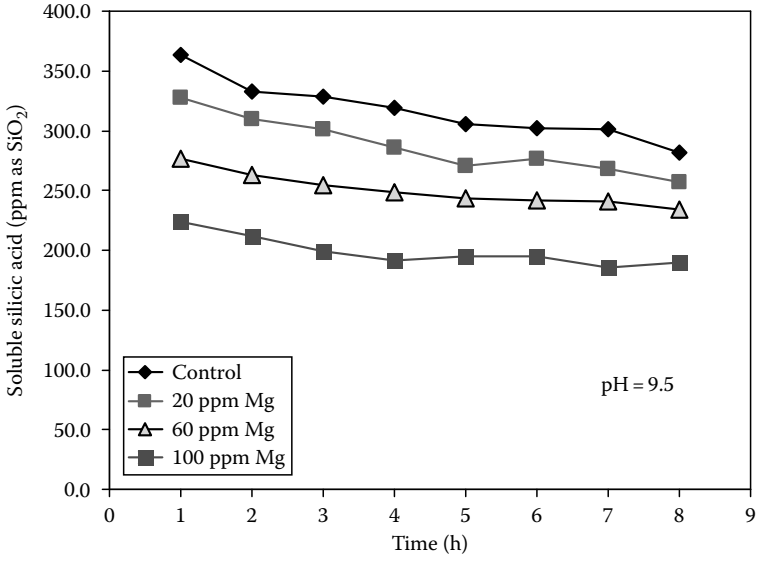

FIGURE 10.15 The effect of Mg level on silica polymerization at pH 9.5.

$$Fe^{3+} + Si(OH)_4 + H_2O \rightarrow [FeSiO(OH)_3]^{2+} + H_3O^+ \quad (10.1)$$

The experimental pH covered was <3.5, however it is expected that similar interactions take place in natural water pH. They found that the stability constant for the Fe(III)-silicate complex is 1.8×10^9. Increased silica concentrations accelerated Fe(II) to Fe(III) oxidation in pH ranges 6.6–7.1 [32]. Fe(III) has a higher propensity for silicate or colloidal silica than Fe(II). This may create iron (III) silicate precipitates. Chan et al. studied the effect of Fe^{3+} on silica fouling of a pilot heat exchanger [33]. Experiments were performed at 125°C–165°C, 1.58 MPa and under turbulent conditions. It was shown that the addition of a few ppm Fe^{3+} into a silica solution was sufficient to induce coagulation

and deposition of silica particles. These in turn caused a significant increase in fouling rates. Gallup studied iron silicate formation and its inhibition in geothermal systems [34].

10.9.2 Aluminum Silicate

Siliceous scales deposited from geothermal brines often contain co-deposited Fe and Al. Fe and Al-rich amorphous silica scales have been reported to form from geothermal brines in Iceland; Japan; Greece; Djibouti; Salton Sea, California; Coso Hot Springs, California; and Dixie Valley, Nevada [35]. The concentrations of Al and SiO_2 in brines depositing scale range from 0.1 to 1 and 600 to 900 ppm, respectively. The scales consist primarily of Al-rich SiO_2. Al/Si molar ratios typically range from 0.1 to 0.2. Traces of Fe, alkalis, and alkaline earth metals were also found. Based on XRD, NMR, and FT-IR measurements, it was concluded that Al is four-coordinate in an opal-like framework [36]. Although Al retards *silicic acid* polymerization, in the near-neutral pH range [37], it is observed to concentrate in siliceous geothermal scales [38].

Amorphous aluminum-rich silica has been identified as a primary scale constituent deposited from certain geothermal brines. This scale is a non-stoichiometric compound exhibiting an empirical formula approaching $Al_2O_3 \cdot (10–20)SiO_2$, and consists of aluminum incorporated in an amorphous silica matrix. Spectroscopic studies indicate that aluminum is coordinated with silica in a three-dimensional array of corner-sharing tetrahedra. Aluminum in scale appears to derive from brine as a result of a reaction with silicic acid oligomers. There is no evidence to suggest that the scale is a simple mixture of amorphous alumina and silica, or a mixture of molecularly deposited silica and aluminosilicate minerals transported in brine from the reservoir. The Al-rich scale tends to deposit from brine at a higher temperature than that of pure amorphous silica. In laboratory experiments, aluminum reacts with supersaturated silicic acid solutions over the pH range 5–9 to precipitate aluminum and silica. The concentrations of aluminum and silica in the mixtures reach a minimum at near-neutral pH. Laboratory experiments indicate that aluminum-silica precipitation reactions are inhibited below pH 5 and above pH 9. A schematic presentation of the structural details of aluminum silicate is shown in Figure 10.16.

Amorphous aluminosilicate is one of the essential components in geochemical processes, such as weathering [39] and adsorption phenomena [40]. In natural systems, amorphous aluminosilicates are formed mainly by the co-precipitation of silicic acid and aluminum hydroxide [41]. There is a strong pH-dependent reaction between silica sols and Al^{3+} [42]. For example, 1 ppm of Al^{3+} is sufficient to reduce 45 ppm SiO_2 in the sol to 5 ppm in the pH range 4–5. Soluble SiO_2 requires considerably larger ratios of Al^{3+} to precipitate the silica at an optimum pH of 8–9 [43].

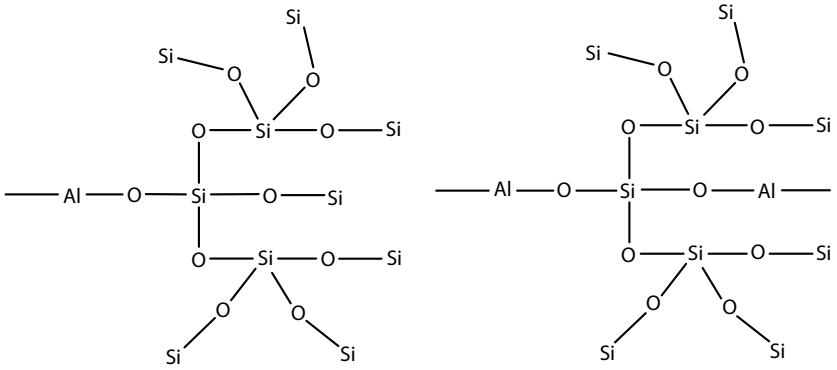

FIGURE 10.16 Schematic three-dimensional structures of aluminum silicate.

10.9.3 Calcium Silicate

Calcium silicate hydrate (CSH) is the major product of Portland cement hydration, where it forms as an amorphous phase of variable composition. CSH is thought to form a layered structure related to tobermorite and jennite [44]. FT-IR of CSH is very similar to that of silica [45].

10.10 EFFECT OF OTHER CATIONS

Studies on the effects of Na^+ and K^+ on silica fouling of heat exchangers under turbulent flow conditions were carried out. It was found that the silica fouling rate in the presence of Na^+ is greater than that when K^+ is present [46]. The effect of cations on decreasing silica solubility follows the order $Mg^{2+} > Ca^{2+} > Li^+ > Na^+ > K^+$ [47,48]. At pH 7, Cu^{2+} ions are absorbed on a SiO_2 surface as polymeric hydroxide species [49]. The structure of these species is similar to that of the bulk amorphous $Cu(OH)_2$. The amorphous state of the supported $Cu(OH)_2$ is caused by a small size (11 Å) of the surface particles. In contrast, the overstoichiometric water molecules seem to have an effect of making bulk $Cu(OH)_2$ more amorphous.

10.11 MAGNESIUM HYDROXIDE AND ITS ROLE IN MAGNESIUM SILICATE FORMATION

Our discussion on metal silicates also involves $Mg(OH)_2$. This is because its role has been invoked before in the formation and growth of magnesium silicate [50]. The region of $Mg(OH)_2$ insolubility is from pH 9.2 upward [51]. Aspects of magnesium hydroxide chemistry have been utilized in removing silica from process water streams. Other than anion resins, Mg^{2+} has been the most commonly used reagent to remove silica from water [52]. It was shown that for a saturated amorphous SiO_2 solution with about 140 ppm silica content, with an equivalent amount of $MgCl_2$ added, the maximum precipitation is at pH 11–11.5. About 35 ppm of SiO_2 remains in the solution [53]. Another report also showed that the addition of 100 ppm of "active" MgO can reduce silica content at 93°C from 22 to 1 ppm [54]. However, at 30°C the reduction is only 16 ppm. A common method of water "softening" is the hot-lime process in which lime (or dolomitic lime) and soda ash are added to water preheated with steam. Such a system is often used to remove silica. Temperature has a profound effect on silica removal [55]. A practical set of curves from Nordell shows the relation between silica present and magnesium added for removal. These curves include a 15% safety factor. Although this method seems to be effective, there are some disadvantages: (a) high temps are required for effective silica removal, (b) circulation of sludge and cold influent is required for maximum reaction with silica, and (c) high cost.

In the desalination of brackish water, silica is one of the major foulants that forms on the reverse osmosis membranes and limits the water recovery. In addition, it is a very adherent scale and once it forms, it is very difficult to clean and cleaning may damage the membrane. There are also complicating factors affecting silica fouling, such as the presence of cations (e.g., Ca, Mg, etc.) that usually promote silica polymerization. Pretreatment is used as a measure to reduce silica levels in the feed and hence mitigate silica fouling. Silica removal was also tested in the presence of sodium aluminate, lime, and soda ash in laboratory tests using field waters [56].

10.12 EFFECT OF ADDITIVES ON METAL SILICATE SCALE CONTROL

Since waterborne metal silicates are amorphous "binary systems," the use of "traditional" threshold scale inhibitors is expected to be ineffective. However, control strategies that are based on either eliminating the metal cation or stabilizing silicic acid in its soluble form have a realistic

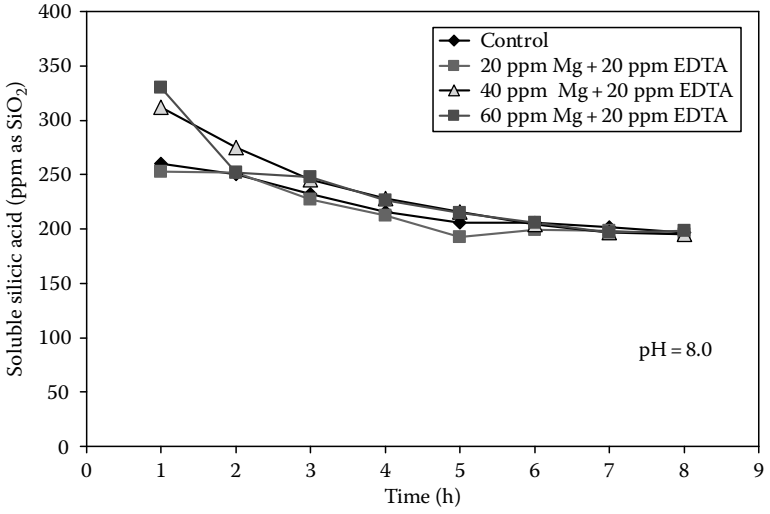

FIGURE 10.17 Influence of EDTA dosage on inhibiting the catalytic effect of Mg^{2+} on silicic acid polymerization at pH 8.0.

chance of being successful. Laboratory studies show that sequestering agents such as citric, acetic, and EDTA acids inhibit aluminum silicate scale formation in geothermal water systems [35]. Aluminum silicate scale deposition may be controlled at these pH extremes with precaution against corrosion and by-product scale formation. Low concentrations of complexing/sequestering agents with a carboxylate functionality maintain aluminum and silica in solution. These results imply that aluminum silicate scaling may be controlled by the treatment of brine with agents that form complexes with aluminum. Bulk silica precipitation can be successfully inhibited by brine pH adjustment alone. When residual aluminum-rich, amorphous silica scaling is to be prevented, the treatment of brines with low dosages of aluminum complexing agents may be necessary. Combinations of complexing agents and brine pH adjustment or the use of acidic complexing agents may prove useful in controlling amorphous aluminum-rich silica scale deposition from geothermal brines.

Magnesium silicate scale control was pursued in our laboratories by the use of EDTA as a Mg sequestering agent. Figure 10.17 shows that the addition of EDTA at a ppm level equal to that of Mg has no effect on soluble silicic acid. These experiments were performed by monitoring soluble silicic acid levels (starting concentration of silicic acid was 500 ppm as SiO_2). EDTA was proven to be ineffective at the dosages shown. Soluble silicic acid levels were the same as those without the presence of EDTA.

When the operational pH was increased to 9.0, the same situation was observed. As illustrated in Figure 10.18, no increase in soluble silicic acid levels is observed and these silicic acid values are the same as those without EDTA present.

When the pH was increased to 9.5, a profound, dosage-dependent effect of EDTA was observed (Figure 10.19). All three EDTA dosages (20, 40, and 60 ppm) caused soluble silicic acid above the control. An interesting observation warrants further discussion. The dosage dependence seems to have an inverse relationship. The higher the Mg/EDTA combination dosage, the lower soluble silica is observed. Therefore, the most effective Mg/EDTA combination for maximum soluble silica is 20/20 ppm. A possible explanation for this inverse effect may be that at increased Mg/EDTA levels (40/40 and 60/60 ppm), the possible precipitation of a Mg-EDTA complex may be occurring. EDTA is well known to be an effective chelator of Mg at high pH regions. A Mg-EDTA complex has been structurally characterized [57].

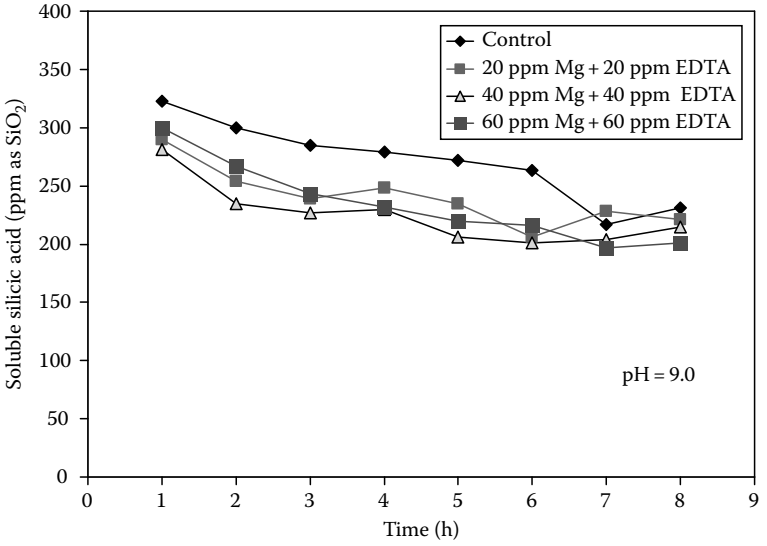

FIGURE 10.18 Influence of EDTA dosage on inhibiting the catalytic effect of Mg^{2+} on silicic acid polymerization at pH 9.0.

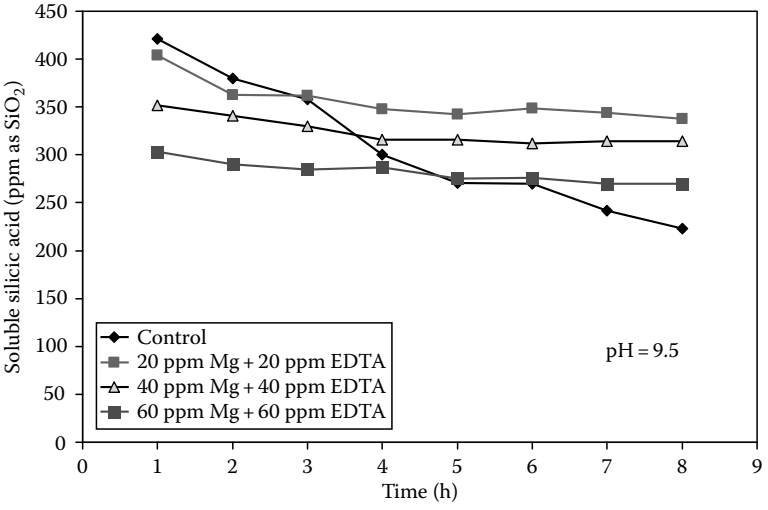

FIGURE 10.19 Influence of EDTA dosage on inhibiting the catalytic effect of Mg^{2+} on silicic acid polymerization at pH 9.5.

10.13 PRACTICAL GUIDELINES FOR CONTROL OF MAGNESIUM SILICATE SCALE

Previously, rough guidelines (summarized in Table 10.2) were based on multiplying the magnesium hardness with the silica concentration. If the product was below 20,000, the water was considered stable. A more advanced rule of thumb was to set the maximum at 40,000 when the pH was below 7.5. Even this was only an approximation, and did not account for the temperature effects. The magnesium silicate system is quite complicated. Several solid compounds of different stoichiometries and hydration states are well known. Magnesium also forms stable complexes with the $(OH)_3SiO^-$ anion as well as the hydroxide ion. This is an addition to the already complicated chemistry of silica

TABLE 10.2
Rough Guidelines for Magnesium Silicate Control

pH Region	$Mg^a \times SiO_2^a$	SiO_2^a	Comments
<7.5	Mg × SiO_2 should be below 40,000 ppm^2	Reactive SiO_2 should be below ~200 ppm	Magnesium silicate usually does not precipitate
>7.5–8.5	Mg × SiO_2 should be below 12,000 ppm^2	Reactive SiO_2 should be below ~150 ppm	Onset of magnesium silicate precipitation possible
>8.5	Mg × SiO_2 should be below 3,000 ppm^2	Reactive SiO_2 should be below ~100 ppm	"High-risk" pH region for magnesium silicate precipitation

[a] Mg is expressed in ppm as $CaCO_3$ and SiO_2 as ppm SiO_2.

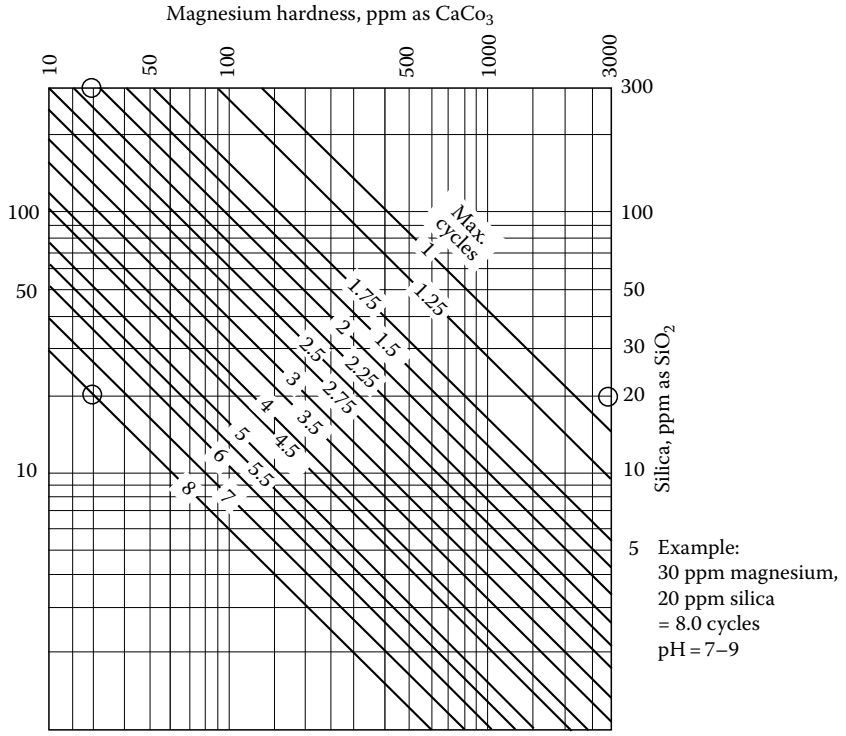

FIGURE 10.20 Correlation between magnesium hardness and silica in process waters in calculating maximum cycles of concentration.

alone. All these factors influence the precipitation of magnesium silicate. Guidelines for the proper operation of the cooling tower under high concentrations of magnesium and silica have been set (see Figure 10.20).

10.14 "METAL SILICATES" IN BIOLOGICAL SYSTEMS

Calcium and iron are found in mineral phases and biopolymers next to silica within biomineralized structures. Silicon can affect the mineralization of both iron oxide and calcium phosphate phases by solution or solid-state interactions. Silicon also appears to have a direct relationship

with aluminum in mineralized pathological deposits. In summary, it can be clearly seen that "silicon"–metal interactions not only occur, but they are an important part of biological processes. Significant studies have been published on the molecular nature of the silicon–metal interactions and in particular on which species (silicon-containing and metal-containing) are involved in such processes [58]. Results indicated that Al^{3+} and orthosilicic acid/silica are able to interact under conditions relevant to biological systems. The inclusion of aluminum in silica, even at the highest Si:Al ratio, also demonstrates the strong affinity between these elements. This is because silicic acid is able to compete successfully with other strong ligands for the metal cation. In a different paper, Perry et al. showed that the use of complexing/sequestering agents for aluminum to prevent the formation of the aluminum-rich silica scale may not be as feasible an option as originally thought [59].

It was reported that the complex formed between aluminum and oligomeric silica has a log Keff of 11.70. This affinity for aluminum is at least 1 million times greater than that for monomeric silica). Another important observation is that aluminum stabilizes silica oligomers for several days under conditions in which depolymerization would otherwise be complete within 24 h. In contrast, oligomeric silica diluted in the absence of aluminum, fully deoligomerized by 24 h, and lost its aluminum binding capacity. Under physiological conditions, this soluble oligomeric silica competes effectively for aluminum with the endogenous chelator citrate. Clearly, the oligomeric-silica/aluminum interaction is of high affinity, and work demonstrating the biological activity of soluble silica should carefully distinguish between monomeric and oligomeric forms.

10.15 EPILOGUE

Silica polymerization is governed largely by pH. Unfortunately, silica is a recalcitrant foulant that is not easily mitigated by simple operational pH adjustments. For example, $CaCO_3$ scale can virtually be eliminated if a cooling tower system is operated at a lower pH. With water containing a high concentration of silica, operation at a higher pH generates the problem of magnesium silicate scale. Lowering the pH (by feeding acid) does not eliminate the problem, it just shifts the "high risk" from magnesium silicate to silica. In contrast to "traditional" mineral scales such as $CaCO_3$, threshold inhibitors (usually phosphonates) are not active for silica scale [60].

An added requirement that is recently gaining a lot of attention is that chemical additives for scale inhibition must be nontoxic, environmentally friendly, and biodegradable. This approach is gaining more governmental and public approval, but is certainly a challenge for chemists and water technologies that are active in the field of chemical water treatment. In the quest for the discovery, application, and commercialization of new silica and metal silicate scale inhibitors, Nature may play an important role in revealing how high levels of silicic acid are stabilized within the diatom. New information may lead to novel synthetic polymers in a biomimetic approach [61]. Until then, research in this field will be active.

ACKNOWLEDGMENTS

A number of hardworking students and enthusiastic collaborators have greatly contributed to the research described herein. A sincere "thank you" goes to my past and current students Eleftheria Neofotistou, Eleftheria Mavredaki, Anna Tsistraki, Kostas Pachis, Stella Katarachia, Antonia Ketsetzi, Aggeliki Stathoulopoulou, Panos Lykoudis, and my collaborators Prof. Petros G. Koutsoukos (University of Patras, Greece), Dr. Viviana Ramos (Universidad Complutense, Spain), and Dr. Adriana Popa (Romanian Academy of Sciences, Romania). This research was funded by the General Secretariat of Science and Technology (Ministry of Development) under Grants GSRT 170c and PEPER-2006 (Crete Prefecture).

REFERENCES

1. (a) Bott, T.R. *Fouling Notebook*, Institution of Chemical Engineers, Rugby, U.K. (1990); (b) Cowan, J.C. and Weintritt, D.J. *Water-Formed Scale Deposits*, Gulf Publishing Company, Houston, TX (1976); (c) Amjad, Z. *Mineral Scale Formation and Inhibition*, Plenum Press, New York (1995); (d) Bott, T.R. *Fouling of Heat Exchangers*, Elsevier Science, Amsterdam, the Netherlands (1995); (e) Chan, S.H., Heat and mass transfer in fouling, in *Annual Review of Heat Transfer*, Begell House, Inc., New York (1992), pp. 363–402.
2. (a) Frenier, W. *Technology for Chemical Cleaning of Industrial Equipment*, NACE, Houston, TX (2000); (b) Demadis, K.D. and Mavredaki, E., Green additives to enhance silica dissolution during water treatment. *Environ Chem Lett* 3, 127–131 (2005); (c) Frenier, W.W. and Barber, S.J., Choose the best heat exchanger cleaning method. *Chem Eng Prog* 94, 37–44 (July, 1998).
3. (a) Brözel, V.S. and Cloete, T.E. Resistance of bacteria from cooling waters to bactericides. *J Ind Microbiol* 8, 273–276 (1991); (b) Saad, M.A. Biofouling prevention in RO polymeric membrane systems. *Desalination* 88, 85–105 (1992); (c) Vrouwenvelder, J.S., Manolarakis, S.A., Veenendaal, H.R., and van der Kooij, D. Biofouling potential of chemicals used for scale control in RO and NF membranes. *Desalination* 132, 1–10 (2000).
4. Demadis, K.D., Yang, B., Young, P.R., Kouznetsov, D.L., and Kelley, D.G. Rational development of new cooling water chemical treatment programs for scale and microbial control. In *Advances in Crystal Growth Inhibition Technologies*, Amjad, Z. (Ed.), Plenum Press, New York (2000), Chapter 16, pp. 215–234.
5. (a) Mann, S. and Perry, C.C. In *Silicon Biochemistry,* Ciba Foundation Symposium 121, Evered, D. and O'Connor, M. (Eds.), John Wiley & Sons Ltd., New York (1986); (b) Tacke, R. Milestones in the biochemistry of silicon: From basic research to biotechnological applications. *Angew Chem Int E* 38, 3015–3018 (1999).
6. (a) Iler, R.K. *The Chemistry of Silica (Solubility, Polymerization, Colloid and Surface Properties and Biochemistry)*, Wiley-Interscience, New York (1979); (b) Fournier, R.P. The solubility of amorphous silica in water at high temperatures and high pressures. *Am Mineral* 62, 1052–1056 (1977); (c) Weres, O., Yee, A., and Tsao, L. Kinetics of silica polymerization. *J Colloid Interface Sci* 84, 379–402 (1981); (d) Sjöberg, S. Silica in aqueous environments. *J Non-Cryst Solids* 196, 51–57 (1996).
7. Bergna, H.E. In *The Colloid Chemistry of Silica*, Bergna, H.E. (Ed.), American Chemical Society, Washington DC (1994).
8. Demadis, K.D., Water treatment's "Gordian Knot". *Chem Process* 66(5), 29–32 (2003).
9. (a) Kroger, N., Lorenz, S., Brunner, E., and Sumper, M. Self-assembly of highly phosphorylated silaffins and their function in biosilica morphogenesis. *Science* 298, 584–586 (2002); (b) Morse, D.E. Silicon biotechnology: Harnessing biological silica production to construct new materials. *Trends Biotechnol* 17, 230–232 (1999); (c) Simpson, T.L. and Volcani, B.E. (Eds.), *Silicon and Siliceous Structures in Biological Systems*, Springer-Verlag, New York (1981).
10. (a) Harfst, W. Treatment methods differ for removing reactive and unreactive silica. *Ultrapure Water*, 59–63 (April, 1992); (b) Den, W. and Wang, C.-J. Removal of silica from brackish water by electrocoagulation pretreatment to prevent fouling of reverse osmosis membranes. *Sep Purific Technol* 59, 318–325 (2008); (c) Sheikholeslami, R. and Bright, J. Silica and metals removal by pretreatment to prevent fouling of reverse osmosis membranes. *Desalination* 143, 255–267 (2002); (d) Drucker, J.R., Brodie, D., and Dale, J. Removal of colloids by the use of ion exchange resins. *Ultrapure Water* December, 14–17 (1988); (e) Nakamura, M., Kosaka, K., and Shimizu, H. Process for the removal of silica in high purity water systems. *Ultrapure Water* 31–37 (December, 1988).
11. (a) Yu, H., Sheikholeslami, R., and Doherty, W.O.S. Mechanisms, thermodynamics and kinetics of composite fouling of calcium oxalate and amorphous silica in sugar mill evaporators—A preliminary study. *Chem Eng Sci* 57, 1969–1978 (2002); (b) Yu, H., Sheikholeslami, R., and Doherty, W.O.S. Composite fouling of calcium oxalate and amorphous silica in sugar solutions. *Ind Eng Chem Res* 42, 904–910 (2003).
12. (a) Amjad, Z., Zibrida, J.F., and Zuhl, R.W. Silica control technology for reverse osmosis systems. *Ultrapure Water* 16(2), 35–41 (1999); (b) Amjad, Z. (Ed.), *Reverse Osmosis: Membrane Technology, Water Chemistry, and Industrial Applications*, Van Nostrand Reinhold Publishing Company, New York (1992); (c) Sheikholeslami R., *Fouling of Membrane and Thermal Units: A Unified Approach. Its Principles, Assessment, Control and Mitigation*, 1st edn., Balaban Publishers, Italy (2007); (d) Freeman, S.D.N. and Majerle, R.J. Silica fouling revisited. *Desalination* 103, 113–115 (1995).

13. Amjad, Z., Zibrida, J.F., and Zuhl, R.W. A new antifoulant for controlling silica fouling in reverse osmosis systems. In *International Desalination Association World Congress on Desalination and Water Reuse*, October 6–9, 1997, Madrid, Spain.
14. (a) Gill, J.S. Inhibition of silica-silicate deposit in industrial waters. *Coll Surf A Physicochem Eng Aspects* 74, 101–106 (1993); (b) Gill, J.S. Silica scale control. *Mater Perform* 37, 41–45 (1998).
15. (a) Hann, W.M. and Robertson, S.T., Control of iron and silica with polymeric dispersants, *International Water Conference* 1990, Paper No. 29, pp. 315–329; (b) Hann, W.M., Robertson, S.T., and Bardsley, J.H. Recent experiences in controlling silica and magnesium silicate deposits with polymeric dispersants. *International Water Conference* 1993, Paper No. 59, pp. 358–370; (c) Hann, W.M. and Robertson, S.T., Control of iron and silica with polymeric dispersants, *Ind Water Treatment* 23(6), 12–24 (November/December, 1991).
16. Weng, P. F. Silica scale inhibition and colloidal silica dispersion for reverse osmosis systems. *Desalination* 103, 59–67 (1995).
17. (a) Demadis, K.D. and Neofotistou, E. Inhibition and growth control of colloidal silica: Designed chemical approaches, *Mater Perform*, 38–42 (April, 2004); (b) Neofotistou, E. and Demadis, K.D., Silica scale growth inhibition by polyaminoamide STARBURST® dendrimers. *Coll Surf A Physicochem Eng Aspects* 242, 213–216 (2004); (c) Neofotistou, E. and Demadis, K.D. Use of antiscalants for mitigation of silica fouling and deposition: Fundamentals and applications in desalination systems. *Desalination* 167, 257–272 (2004); (d) Demadis, K.D., Neofotistou, E., Mavredaki, E., Tsiknakis, M., Sarigiannidou, E.M., and Katarachia, S.D. Inorganic foulants in membrane systems: Chemical control strategies and the contribution of "Green Chemistry". *Desalination* 179, 281–295 (2005); (e) Demadis, K.D. A structure/function study of polyaminoamide dendrimers as silica scale growth inhibitors, *J Chem Technol Biotechnol* 80, 630–640 (2005), (f) Demadis, K.D. and Stathoulopoulou, A. Solubility enhancement of silicate with polyamine/polyammonium cationic macromolecules: Relevance to silica-laden process waters. *Ind Eng Chem Res* 45, 4436–4440 (2006); (g) Demadis, K.D. Focus on operation & maintenance: Scale formation and removal. *Power* 148(6), 19–23 (2004); (h) Stathoulopoulou, A. and Demadis, K.D. Enhancement of silicate solubility by use of "green" additives: Linking green chemistry and chemical water treatment. *Desalination* 224, 223–230 (2008); (i) Demadis, K.D., Ketsetzi, A., Pachis, K., and Ramos, V.M. Inhibitory effects of multicomponent, phosphonate-grafted, zwitter-ionic chitosan biomacromolecules on silicic acid condensation. *Biomacromolecules* 9, 3288–3293 (2008); (j) Ketsetzi, A., Stathoulopoulou, A., and Demadis, K.D. Being "green" in chemical water treatment technologies: Issues, challenges and developments. *Desalination* 223, 487–493 (2008).
18. Euvrard, M., Hadi, L., and Foissy, A. Influence of PPCA (phosphinopolycarboxylic acid) and DETPMP (diethylenetriaminepentamethylenephosphonic acid) on silica fouling. *Desalination* 205, 114–123 (2007).
19. (a) Kinrade, S.D. and Swaddle, T.W. Silicon-29 NMR studies of aqueous silicate solutions. 2. Transverse ^{29}Si relaxation and the kinetics and mechanism of silicate polymerization. *Inorg Chem* 27, 4259–4264 (1988); (b) Radzig, V.A. Reactive silica: A new concept of the structure of active sites. *Coll Surf A: Physicochem Eng Aspects* 74, 91–100 (1993); (c) Dove, P.M. and Rimstidt, J.D. Silica-water interactions. Physical behaviour, geochemistry and materials applications. *Rev Mineral* 29, 259–308 (1994); (d) Van Blaaderen, A., Van Geest, J., and Vrij, A. Monodisperse colloidal silica spheres from tetraalkoxysilanes: Particle formation and growth mechanism. *J Colloid Interface Sci* 154, 481–501 (1992).
20. Demadis, K.D. and Neofotistou, E. Synergistic effects of combinations of cationic polyaminoamide dendrimers/anionic polyelectrolytes on amorphous silica formation: A bioinspired approach. *Chem Mater* 19, 581–587 (2007).
21. (a) Dubin, L. Silica stabilization in cooling water systems, in *Surface Reactive Peptides and Polymers: Discovery and Commercialization*, Sikes, C.S. and Wheeler, A.P. (Eds.), American Chemical Society, Washington DC, (1991), pp. 355–379; (b) Meier, D.A. and Dubin, L.A. Novel Approach to silica scale inhibition, CORROSION/87, Paper No. 344, NACE International, Houston, TX (1987); (c) Dubin, L., Dammeier, R.L., and Hart, R.A. Deposit control in high silica water. *Mater Perform* 24(10), 27–33 (1985).
22. Kristmanndóttir, H., Ólafsson, M., and Thórhallsson, S. Magnesium silicate scaling in district heating systems in Iceland. *Geothermics* 18, 191–198 (1989).
23. Kent, D.B. and Kastner, M. Mg^{2+} removal in the system Mg^{2+}-amorphous SiO_2–H_2O by adsorption and Mg-hydroxysilicate precipitation. *Geochim Cosmochim Acta* 49, 1123–1136 (1985).
24. Smith, C.W., Usage of a polymeric dispersant for control of silica. *Ind Water Treat* 4, 20–26 (July/August, 1993).
25. Sheikholeslami, R. and Tan, S. Effects of water quality on silica fouling of desalination plants. *Desalination* 126, 267–280 (1999).

26. (a) Young, P.R. Magnesium silicate precipitation. CORROSION/93, Paper No. 466, NACE International, Houston, TX (1993); (b) Brooke, M. Magnesium silicate scale in circulating cooling systems. CORROSION/84, Paper No. 327, NACE International, Houston, TX (1984).
27. MacKenzie, F.T., Garrels, R.M., Bricker, O.P., and Bickley, F. Silica in sea water: Control by silica minerals. *Science* 155, 1404–1405 (1967).
28. Kristmanndóttir, H. Types of scaling occuring by geothermal utilization in Iceland. *Geothermics* 18, 183–190 (1989).
29. Mattson, S. The laws of soil colloidal behavior. XI. Electrodialysis in relation to soil processes. *Soil Sci* 16, 149–156 (1933).
30. Hazel, F., Schock, R., and Gordon, M. Interaction of ferric ions with silicic acid. *J Am Chem Soc* 71, 2256–2257 (1949).
31. Weber, W.J. and Stumm, W. Formation of a silicato-iron (III) complex in dilute aqueous solution. *J Inorg Nucl Chem* 27, 237–239 (1965).
32. (a) Schenk, J.E. and Weber, W.J. Chemical interactions of dissolved silica with Fe(II) and Fe(III). *J Am Water Works Assoc* 60, 199 (February, 1968); (b) O'melia, C.R. and Stumm, W. Aggregation of silica dispersions by Fe(III). *J Colloid Interface Sci* 23, 437–447 (1967).
33. Chan, S.H., Chen, Z.J., and He, P. Effect of ferric chloride on silica fouling. *J Heat Transfer* 117, 323–328 (1995).
34. (a) Gallup, D.L. Iron silicate formation and inhibition at the Salton Sea geothermal field. *Geothermics* 18, 97–103 (1989); (b) Gallup, D.L. The influence of iron on the solubility of amorphous silica in hypersaline geothermal brines. In *Proceedings of 1991 Symposium on Chemistry in High-Temperature Aqueous Solutions*, Provo, UT.
35. (a) Yokoyama, T., Sato, Y., Maeda, Y., Tarutani, T., and Itoi, R. Siliceous deposits formed from geothermal water. I. The major constituents and the existing states of iron and aluminum. *Geochem J* 27, 375–384 (1993); (b) Yokoyama, T., Sato, Y., Nakai, M., Sunahara, K., and Itoi, R. Siliceous deposits formed from geothermal water in Kyushu, Japan: II. Distribution and state of aluminum along the growth direction of the deposits. *Geochem J* 33, 13–18 (1999); (c) Benevidez, P.J., Mosby, M.D., Leong, J.K., and Navarro, V.C. Development and performance of the Bulalo geothermal field. In *Proceedings of the 10th New Zealand Geothermal Workshop*, Auckland, New Zealand (1988), pp. 55–60; (d) Gunderson, R.P., Dobson, P.F., Sharp, W.D., Pudjianto, R., and Hasibuan, A. Geology and thermal features of the Sarulla contract area, North Sumatra, Indonesia. In *Proceedings of World Geothermal Congress*, Vol. 2, Florence, Italy (1995), p. 687; (e) Gallup, D.L. Aluminum silicate scale formation and inhibition (2): Scale solubilities and laboratory and field inhibition tests. *Geothermics* 27, 485–501 (1998); (f) Gallup, D.L. Aluminum silicate scale formation and inhibition: Scale characterization and laboratory experiments. *Geothermics* 26, 483–499 (1997).
36. Manceau, A., Ildephonse, P., Hazemann, J.-L., Flank, A.-M., and Gallup, D.L. Crystal chemistry of hydrous iron silicate scale deposits at the Salton Sea geothermal field. *Clays Clay Minerals* 43, 304–317 (1995).
37. (a) Yokoyama, T., Takahashi, Y., and Tarutani, T. Retarding and accelerating effects of aluminum on the growth of polysilicic acid particles. *J Colloid Interface Sci* 141, 559–563 (1991); (b) Yokoyama, T., Takahashi, Y., Yamanaka, C., and Tarutani, T. Effect of aluminum on the polymerization of silicic acid in aqueous solution and the deposition of silica. *Geothermics* 18, 321–326 (1989).
38. Yokoyama, T., Sato, Y., Maeda, Y., and Tarutani, T. Elements concentrated into siliceous deposit formed from geothermal water and their distribution. In *Proceedings of the 9th New Zealand Geothermal Workshop*, Auckland, New Zealand (1987), p. 69.
39. (a) Nugent, M.A., Brantley, S.L., Pantano, C.G., Maurice, P.A. The influence of natural mineral coatings on feldspar weathering. *Nature* 395, 588–591 (1998). (b) Ugolini, F.C. and Dahlgren, R.A. Weathering environments and occurrence of imogolite/allophane in selected Andisols and Spodosols. *Soil Sci Soc Am J* 55, 1166–1171 (1991).
40. Miyazaki, A. and Tsurumi, M. The H^+/Zn^{2+} exchange stoichiometry of surface complex formation on synthetic amorphous aluminosilicate. *J Colloid Interface Sci* 172, 331–334 (1995).
41. (a) Ossaka, J. and Iwai, S. Transformation of allophane to kaolinite under low-grade hydrothermal conditions. *Nature* 201, 1019–1020 (1964); (b) Childs, C.W., Parfitt, R.L., and Newman, R.H. Structural studies of silica springs allophone. *Clay Minerals* 25, 329–341 (1990).
42. Okamoto, G., Okuna, T., and Goto, K. Properties of silica in water. *Geochim Cosmochim Acta* 12, 123–132 (1957).
43. Wohlberg, C. and Buchholz, J.R. Silica in water in relation to cooling tower operation, CORROSION/75, Paper No. 143, NACE International, Houston, TX (1975).
44. Taylor, H.F.W. *Cement Chemistry*, 2nd edn., Thomas Telford, London, U.K. (1997).

45. Matsuyama, H. and Young, J.F. Intercalation of polymers in calcium silicate hydrate: A new synthetic approach to biocomposites. *Chem Mater* 11, 16–19 (1999).
46. Chan, S.H., Chen, Z.J., and He, P. Effects of sodium and potassium chlorides on silica fouling. In *Winter Annual Meeting of the American Society of Mechanical Engineers*, Paper No. 90-WA/HT-1, Dallas, TX (1990).
47. Marshall, W.L. and Warakomski, J.M. Amorphous silica solubilities, II: Effect of aqueous salt solutions at 25°C. *Geochim Cosmochim Acta* 44, 915–917 (1980).
48. (a) Chan, S.H., Neusen, K.F., and Chang, C.T. The solubility and polymerization of amorphous silica in geothermal energy applications. In *Proceedings of 1987 ASME-JSME Thermal Engineering Joint Conference*, Vol. 3, Honolulu, HI (1987), p. 103; (b) Chan, S.H. A review on solubility and polymerization of silica. *Geothermics* 18, 49–56 (1989).
49. (a) Kriventsov, V.V., Kochubey, D.I., Elizarova, G.L., Matvienko, L.G., and Parmon, V.N. The structure of amorphous bulk and silica-supported sopper(II) hydroxides. *J Colloid Interface Sci* 215, 23–27 (1999); (b) Zaporozhets, O., Gawer, O., and Sukhan, V. The interaction of Fe(II), Cu(II) and Ag(I) ions and their complexes with 1,10-phenanthroline adsorbed on silica gel. *Coll Surf A Physicochem Eng Aspects* 147, 273–281 (1999).
50. Young, P.R. Stuart, C.M., Eastin, P.M., and McCormick, M. Silica stabilization in industrial cooling towers: Recent experiences and advances. Cooling Technology Institute Annual Meeting Technical Paper TP93-11 (1993).
51. (a) Liu, S.-T. and Nancollas, G.H. The crystallization of magnesium hydroxide. *Desalination* 12, 75–84 (1973); (b) Chieng, C. and Nancollas, G.H. The crystallization of magnesium hydroxide, a constant composition study. *Desalination* 42, 209–219, (1982).
52. (a) Midkiff, W.S. and Foyt, H.P. Silica scale technology and water conservation. *Mater Perform* 39–42 (August, 1979); (b) Midkiff, W.S. and Foyt, H.P. Silica removal and prevention in high silica cooling waters. *Mater Perform* 17–22 (February, 1978).
53. (a) Nesterchuk, N.I. and Makarova, T.A. The formation of aqueous magnesium silicate in the interaction of solutions of magnesium chloride and sodium metasilicate. *Bull Acad Sci USSR, Div Chem Sci* 19, 2053–2055 (1970); (b) Chen, C.T.A. and Marshall, W.L. Amorphous silica solubilities IV. Behavior in pure water and aqueous sodium chloride, sodium sulfate, magnesium chloride, and magnesium sulfate solutions up to 350°C. *Geochim Cosmochim Acta* 46, 279–287 (1982).
54. Betz, L.D., Noll, C.A., and Maguire, J.J. Removal of silica from water by cold process, *Ind Eng Chem* 32, 1320–1323 (1940).
55. Nordell, E. *Water Treatment for Industrial and Other Uses*, 2nd edn., Reinhold Publishing Company, New York (1961).
56. Sheikholeslami, R., Al-Mutaz, I. S., Tan, S., and Tan, S.D. Some aspects of silica polymerization and fouling and its pretreatment by sodium aluminate, lime and soda ash. *Desalination* 150, 85–92 (2002).
57. Stezowski, J.J., Countryman, R., and Hoard, J.L. Structure of the ethylenediaminetetraacetato-aquomagnesate(II) ion in a crystalline sodium salt. Comparative stereochemistry of the seven-coordinate chelates of magnesium(II), manganese(II), and iron(III). *Inorg Chem* 12, 1749–1754 (1973).
58. Perry, C.C. and Keeling-Tucker, T. Aspects of the bioinorganic chemistry of silicon in conjunction with the biometals calcium, iron and aluminum. *J Inorg Biochem* 69, 181–191 (1998).
59. Perry, C.C. and Keeling-Tucker, T. Model studies of the precipitation of silica in the presence of aluminum; implications for biology and industry. *J Inorg Biochem* 78, 331–339 (2000).
60. (a) Demadis, K.D. Combating heat exchanger fouling and corrosion phenomena in process waters, in *Compact Heat Exchangers and Enhancement Technology for the Process Industries*, Shah, R.K. (Ed.), Begell House Inc., New York (2003); (b) Demadis, K.D. and Katarachia, S.D. Metal-phosphonate chemistry: Preparation, crystal structure of calcium-amino-tris-methylene phosphonate and $CaCO_3$ inhibition. *Phosphorus Sulfur Silicon* 179, 627–648 (2004); (c) Demadis, K.D. and Lykoudis, P. Chemistry of organophosphonate scale growth inhibitors: 2. Physicochemical aspects of 2-phosphonobutane-1,2,4-tricarboxylate (PBTC) and its effect on $CaCO_3$ crystal growth. *Bioinorg Chem Appl* 3, 135–149 (2005).
61. Demadis, K.D., Pachis, K., Ketsetzi, A., and Stathoulopoulou, A. Bioinspired Control of Colloidal silica in vitro by dual polymeric assemblies of zwitterionic phosphomethylated chitosan and polycations or polyanions. *Adv Coll Interf Sci* 151, 33–48 (2009).

Chemical Engineering

THE SCIENCE AND TECHNOLOGY OF INDUSTRIAL WATER TREATMENT

Mineral scale deposits, corrosion, suspended matter, and microbiological growth are factors that must be controlled in industrial water systems. Research on understanding the mechanisms of these problems has attracted considerable attention in the past three decades as has progress concerning water treatment additives to ameliorate these concerns. **The Science and Technology of Industrial Water Treatment** provides a comprehensive discussion on the topic from specialists in industry and academia.

Topics discussed include:

- The basics of water chemistry
- The characteristics, formation, and control of common mineral scales
- Membrane-based separation processes
- Reverse osmosis systems and scale control in thermal distillation processes
- Corrosion control in cooling, boiler, geothermal, and desalination systems
- The interactions of polyelectrolytes with suspended matter
- Bacterial species commonly encountered in water supplies, including *Legionella*
- Analytical techniques for identifying mineral scales and deposits
- Polymers for treating industrial and wastewater systems
- Monitoring operational parameters and chemicals in water treatment

A valuable addition to the library of academic researchers, this volume will also prove useful to those working not only in the water treatment industry, but also to those in petroleum, textiles, pharmaceuticals, and other areas where purity processes are a significant concern.

IWA Publishing
London • New York

Co-published by IWA Publishing, Alliance House, 12 Caxton Street, London SW1H 0QS, UK
Tel. +44 (0) 20 7654 5500, Fax +44 (0) 20 7654 5555
publications@iwap.co.uk
www.iwapublishing.com

71440

CRC Press
Taylor & Francis Group
an **informa** business
www.crcpress.com

6000 Broken Sound Parkway, NW
Suite 300, Boca Raton, FL 33487
270 Madison Avenue
New York, NY 10016
2 Park Square, Milton Park
Abingdon, Oxon OX14 4RN, UK

ISBN: 978-1-4200-7144-3
90000
9 781420 071443